N-terminal acetylation separately promotes nuclear localization and host shutoff activity of the influenza A virus ribonuclease PA-X

Raecliffe E. Daly[1,2], Idalia Myasnikov[2], Marta Maria Gaglia[2]

[1] Program in Cellular, Molecular and Developmental Biology, Tufts University Graduate School of Biomedical Sciences, Boston, MA, 02111, United States.

[2] Institute for Molecular Virology and Department of Medical Microbiology and Immunology, University of Wisconsin – Madison, Madison, WI, 53706, United States.

Correspondence: marta.gaglia@wisc.edu

Short title: The multifaceted role of N-terminal acetylation in influenza PA-X function

Abstract

To counteract host antiviral responses, influenza A virus triggers a global reduction of cellular gene expression, a process termed “host shutoff.” A key effector of influenza A virus host shutoff is the viral endoribonuclease PA-X, which degrades host mRNAs. While many of the molecular determinants of PA-X activity remain unknown, a previous study found that N-terminal acetylation of PA-X is required for its host shutoff activity. However, it remains unclear how this co-translational modification promotes PA-X activity. Here, we report that PA-X N-terminal acetylation has two functions that can be separated based on the position of the acetylation, i.e. on the first amino acid, the initiator methionine, or the second amino acid following initiator methionine excision. Modification at either site is sufficient to ensure PA-X localization to the nucleus. However, modification of the second amino acid is not sufficient for host shutoff activity of ectopically expressed PA-X, which specifically requires N-terminal acetylation of the initiator methionine. Interestingly, during infection N-terminal acetylation of PA-X at any position results in host shutoff activity, which is in part due to a functional interaction with the influenza protein NS1. This result reveals an unexpected role for another viral protein in PA-X activity. Our studies uncover a multifaceted role for PA-X N-terminal acetylation in regulation of this important immunomodulatory factor.

Introduction

Although influenza A viruses have a relatively small genome of approximately 13.5 kb, multiple influenza proteins are involved in modulating the host immune response. Of the influenza immunomodulatory proteins identified to date, PA-X has emerged as a key factor in regulating gene expression and innate immune responses. Studies using viruses engineered to lack PA-X have revealed that PA-X limits innate immune and inflammatory responses during infection, which reduces inflammation-induced pathology (1,2). Immune regulation by PA-X is the result of its crucial role in influenza host shutoff, i.e. the global reduction of gene expression during infection(1,3,4). PA-X is an endoribonuclease (endoRNase)(1,4,5), and it carries out host shutoff by degrading host mRNAs, while largely sparing viral RNAs(4,6). While previous studies by us and others have dissected the specificity of RNA targeting by PA-X, we still have limited information on how PA-X functions. In particular, whether and how PA-X activity is modulated in cells remains unclear.

A study by Oishi et al. in 2018 reported that PA-X is N-terminally acetylated by the host N-terminal acetyltransferase complex B (NatB) while it is being translated(7). Moreover, they showed that this co-translational modification is required for the host shutoff activity of PA-X(7). N-terminal acetylation is a highly abundant protein modification in cells, with 80-90% of the human proteome acquiring this modification during translation(8–11). It is catalyzed by several Nat complexes (NatA-NatF), which differ in their subunit composition and substrate specificity(12,13). The substrate specificity is mainly determined by the first two N-terminal residues of the target protein (12). NatA, NatB, and NatC are responsible for the majority of N-terminal acetylation events in eukaryotes(13). NatB and NatC acetylate nascent polypeptides on the very first translated amino acid, the initiator methionine, while NatA modifications occur following the excision of the initiator methionine by host methionine aminopeptidases. Despite the fact that N-terminal acetylation is a common modification, only a handful of studies have

investigated the effect of N-terminal acetylation on protein function(13,14). Nonetheless, multiple roles for this modification have been described. N-terminal acetylation has been implicated in the control of protein stability(15–19), protein folding(20–22), protein-protein interactions(23–28), and subcellular targeting(29–32). While PA-X requires this modification to function, it remains unknown how N-terminal acetylation supports PA-X host shutoff activity.

A complication in studying PA-X N-terminal acetylation is that PA-X shares its N terminus with the polymerase acidic (PA) subunit of the influenza RNA polymerase, a protein that is essential for viral replication(1,33). This is because PA-X is generated from the same mRNA as PA (the mRNA transcribed from the influenza genomic segment 3) through ribosomal frameshifting after translation of the 191st amino acid of PA(1,33). Therefore, mutations or acetylase knockdown/knockouts that alter PA-X N-terminal acetylation also impact PA N-terminal acetylation(7). Moreover, PA appears to require this modification for its function, also due to an unknown mechanism of regulation(7). Due to this complication, the impact of PA-X N-terminal acetylation during infection was not separated from that of PA modification in the initial study from Oishi et al.(7)

Here, we report that N-terminal acetylation supports PA-X activity by two separate mechanisms. N-terminal acetylation is needed for PA-X nuclear localization, which we and others have shown is required for the host shutoff activity of PA-X(4,34,35). Interestingly, we found that PA-X localizes to the nucleus when modified by Nat complexes that add the modification to either the initiator methionine or the second residue following initiator methionine excision. However, in the absence of viral infection, the localization alone is not enough to confer host shutoff activity, and PA-X specifically requires modification of the initiator methionine to downregulate RNA levels in cells. This result suggests that N-terminal acetylation on the initiator methionine has a separate role in supporting PA-X host shutoff activity. To our surprise, we also observed that PA-X

mutants modified at the second amino residue downregulate transcripts during infection, even though they are largely inactive when PA-X is ectopically expressed. This discrepancy between ectopic expression and infection led us to uncover that the viral protein NS1 promotes the host shutoff activity of PA-X. NS1 appears to rescue RNA downregulation by PA-X mutants with otherwise low activity, suggesting that NS1 and PA-X proteins functionally interact during PA-X-driven host shutoff, as also recently suggested by Bougon et al.(36).

Results

N-terminal acetylation is required for PA-X nuclear localization, but nuclear localization in the absence of acetylation is not sufficient for host shutoff activity

Previous studies using the influenza A/WSN/33 H1N1 (WSN) virus have shown that N-terminal acetylation of PA-X by the NatB complex is important for its host shutoff activity in mammalian cells(7). When the N terminus of PA-X is mutated from ME- to MP- to produce non-acetylated PA-X proteins (Fig. 1A)(13,37), the shutoff activity of PA-X is lost(7). While the functions of N-terminal acetylation have only been described in a handful of studies(15–32), one of the established functions of this modification is control of subcellular localization(29–32). We and others have reported that PA-X must localize to the nucleus to downregulate mRNAs(4,34,35). To determine whether non-acetylated mutants lose activity because of primarily cytoplasmic localization, we compared the subcellular localization of ectopically expressed eGFP-tagged wild-type (WT) PA-X from the influenza A/Puerto Rico/8/1934 H1N1 virus (PR8) and the non-acetylated PR8 PA-X E2P mutant using confocal microscopy. To confirm that the PR8 PA-X E2P mutant loses activity similarly to the WSN PA-X E2P mutant, we co-transfected cells with PA-X and a luciferase reporter and measured luciferase RNA levels by qPCR, as we have done in previous studies(4,5). As expected, the PA-X E2P mutant did not downregulate luciferase mRNA levels, and luciferase levels in PA-X E2P transfected cells were similar to those in cells

transfected with the catalytically inactive PA-X D108A mutant (Fig. 1B)(4,5). To quantify PA-X localization unbiasedly, we computed Manders' overlap coefficients between the PA-X-eGFP signal and Hoechst nuclear staining from confocal microscopy images using the ImageJ plugin Just Another Colocalization Plugin (JACoP)(38). Manders' overlap coefficient values range from 0 to 1. 0 indicates no overlap between the two signals, in this case representing primarily cytoplasmic localization, and 1 indicates complete overlap, in this case representing primarily nuclear localization. eGFP alone showed an average Manders' overlap coefficient of 0.52, indicating diffuse localization throughout cells, and WT PA-X was predominantly nuclear, with an average Manders' overlap coefficient of 0.86, consistent with previous studies(4,34,35). Interestingly, PA-X E2P was more diffusely localized than WT PA-X, and had an average Manders' overlap coefficient of 0.51, similar to eGFP (Fig. 1C,D). These results suggest that N-terminal acetylation is required for the nuclear accumulation of PA-X, which could explain its loss of activity. As a control we also generated two mutants that have a different sequence but should still be modified by NatB, PA-X E2D and PA-X E2N (Fig. 1A). In both the WSN(7) and the PR8 (Fig. 1E) background, these NatB modified mutants had similar host shutoff activity to WT PA-X. Consistent with this result, PA-X E2D and PA-X E2N also had similar localization to WT PA-X (Manders' overlap coefficients = 0.88 and 0.86, respectively, Fig. 1F,G). These results suggest that the differences seen between WT PA-X and PA-X E2P are due to changes in N-terminal acetylation, and not changes in the protein sequence.

To determine whether the decreased activity of PA-X E2P was due only to its change in subcellular localization, we fused PA-X E2P to the canonical SV40 nuclear localization signal(39) to restore nuclear localization. However, PA-X E2P-NLS remained unable to downregulate luciferase mRNA levels (Fig. 1B), indicating that nuclear localization alone is not enough to restore the host shutoff activity of unmodified PA-X. Therefore, to downregulate RNA levels in cells, PA-X also requires N-terminal acetylation for a second function.

N-terminal acetylation at any position is sufficient for PA-X localization to the nucleus, but not for host shutoff activity

To further explore the relationship between PA-X N-terminal acetylation, nuclear localization, and host shutoff activity, we tested a select number of PA-X mutants that are modified by the host complex NatA (Fig. 1A). Unlike NatB-modified proteins, which are N-terminally acetylated at the initiator methionine, NatA-modified proteins are N-terminally acetylated at the second residue following methionine excision (13,40,41) (Fig. 1A). A previous study showed that, like the non-acetylated WSN PA-X E2P mutant, the NatA-modified WSN PA-X E2A mutant loses its host shutoff activity(7), suggesting the initiator methionine needs to be retained for PA-X function. We confirmed that this was also the case with the PR8 PA-X E2A mutant (Fig. 2A). In addition, we generated two additional NatA modified mutants, PA-X E2S and PA-X E2V, which also had no apparent host shutoff activity in cells (Fig. 2A). Despite these differences in activity, the levels of these mutants, as well as those of the PA-X-E2P mutant, appeared similar in microscopy analysis (Fig. 1C, 2B; because of the instability of the PA-X protein(42) we are not consistently able to analyze its expression levels by western blotting). Interestingly, we saw that PA-X E2A and E2S had similar localization to WT PA-X, and primarily accumulated in the nucleus (Fig. 2B,C) despite losing the ability to downregulate luciferase mRNA levels (Fig. 2A). In contrast, PA-X E2V was more diffusely localized between the nucleus and the cytoplasm, similar to the unmodified PA-X E2P (Fig. 1C,D; Fig. 2B,C). For PA-X E2V, this decrease in nuclear localization could be due to the lower levels of N-terminal acetylation reported for proteins that start with MV-(10,41). Taken together, these data suggest that N-terminal acetylation at any position and at high levels is sufficient for PA-X nuclear localization, but that this modification alone is not able to support host shutoff activity.

N-terminal acetylation at the initiator methionine promotes PA-X host shutoff activity

It is surprising that PA-X mutants that are acetylated(7) and localize to the nucleus (Fig. 1B,C) are inactive. A previous study hypothesized that perhaps the NatB complex activity, rather than the modification, was important(7). However, NatA- and NatB-modified proteins also differ in the presence of the initiator methionine and thus the location of the modification (Fig. 1A). To test if the site of the modification was the determining factor for PA-X activity, we investigated the effect of modification by NatC, which, like NatB, also modifies proteins on the initiator methionine(10,13). To do so, we employed two mutants that should be modified by NatC(10,13), PA-X E2M and PA-X E2L (Fig. 1A). The subcellular localization of the NatC-modified mutants was similar to that of WT PA-X (Fig. 3A,B). In addition, the NatC-modified mutants were also able to downregulate luciferase mRNA levels in cells, although to a lesser degree than WT PA-X and the other NatB-modified mutants (Fig. 3C). Thus, N-terminal acetylation of the initiator methionine specifically is required for the host shutoff activity of PA-X.

N-terminal acetylation by various Nat complexes has similar consequences on the activity of PA-X activity of all influenza A strains tested

While results with WSN(7) and PR8 PA-X are suggestive of a broader phenomenon, both of these strains are lab-adapted viruses. Therefore, we sought to ensure that the phenotype of N-terminal acetylation mutants was conserved with PA-X proteins from more relevant human seasonal influenza viruses. Currently circulating seasonal human viruses are H1N1 strains related to the pandemic 2009 H1N1 virus (H1N1pdm09), and H3N2 strains(43). Thus, we tested the effect of E2P (no modification), E2A (modification by NatA), and E2M (modification by NatC) mutations in the PA-X sequences from A/Tennessee/1-560/09 H1N1 (H1N1pdm09) and A/Perth/16/2009 H3N2 (Perth). We found that the trend in host shutoff activity was similar

among PA-X proteins from all influenza A strains tested. All PA-X E2A and PA-X E2P mutants had significantly lower (or no) host shutoff activity, while the PA-X E2M mutants maintained an intermediate amount of activity (Fig. 4). These data suggest that regardless of viral strain, PA-X requires N-terminal acetylation, in general, to access the nucleus and N-terminal acetylation of the initiator methionine specifically to downregulate RNA levels.

N-terminal acetylation at any position is sufficient for the host shutoff activity of PA-X during infection

Our results point to the importance of PA-X N-terminal acetylation for nuclear localization and host shutoff activity when PA-X is ectopically expressed in cells. However, we wanted to confirm that this modification is also important during viral infection. This was not done in the previous study by Oishi et al.(7) because of the challenges in separating PA and PA-X translation during infection. PA-X is produced by a +1 frameshifting event that occurs after translation of the 191st amino acid of PA(1). Therefore, any mutation in the PA-X N terminus is also present in PA because of their identical N termini(1), which is problematic as PA also requires N-terminal acetylation for polymerase activity(34). To separate PA and PA-X production, we examined the activity of ectopically expressed PA-X mutants in cells infected with PA-X-deficient PR8 (PR8 PA(ΔX))(5). To ensure that the experimental set up would work, we first transfected 293T cells with plasmids encoding eGFP or eGFP-tagged WT PA-X, and then either left them uninfected or infected them with WT PR8 or PR8 PA(ΔX). We found that transfecting cells did not prevent them from being infected with WT PR8 or PR8 PA(ΔX) viruses, as all cells expressed similar levels of influenza HA RNAs (Fig. 5A). Moreover, transfection did not inhibit the ability of PA-X to downregulate its endogenous targets, as G6PD, a known target of PA-X(5), was downregulated in transfected cells that were infected with WT PR8 (Fig. 5B). We then repeated the experiment and transfected cells with eGFP-tagged versions of PA-X carrying E2P

(unmodified), E2D (NatB-modified), E2A (NatA-modified), or E2M (NatC-modified) mutations, in addition to WT PA-X and eGFP alone, as well as a luciferase reporter. Cells were then left uninfected or were infected with PR8 PA(ΔX) virus (Fig. 5C). As expected, based on the levels of luciferase mRNA, unmodified PA-X E2P remained inactive during infection, and NatB-modified PA-X E2D maintained host shutoff activity comparable to WT PA-X (Fig. 5C). However, to our surprise, NatC-modified PA-X E2M and NatA-modified PA-X E2A had higher levels of host shutoff activity in infected vs. uninfected cells (Fig. 5C). These results suggest that additional factors during infection enhance the host shutoff activity of PA-X mutants with attenuated host shutoff activity.

The influenza A virus protein NS1 potentiates PA-X activity during infection

A possible reason for the increased host shutoff activity of PA-X E2A during infection is a functional interaction between PA-X and another viral protein. In the past, this possibility has not been heavily investigated, since all studies have indicated that PA-X is active upon ectopic expression in uninfected cells, in the absence of other viral proteins. Also, our previous analyses also suggest that it has similar RNA targets in infected and uninfected cells(4–6). To test the hypothesis that other influenza proteins potentiate PA-X activity, we compared mRNA downregulation by ectopically expressed WT PA-X alone or by the NatA-modified PA-X E2A mutants expressed together with PR8 PB2, PB1, PA, HA, NP, NA, M1, M2, NS1, or NEP (Fig. 6A). To prevent WT PA-X expression from the PA segment, we used a version with a mutation in the frameshift sequence that reduces PA-X production (TTTCGT to TTCCGC, which strongly attenuates the +1 ribosomal frame shift during translation)(44). When PR8 NS1 was co-transfected with PA-X E2A, we observed an increase in host shutoff activity (Fig. 6A,C), whereas co-expression of other PR8 proteins had no effect (Fig. 6A). As some of the PR8 proteins were not expressed at detectable levels (Fig. 6B), we cannot exclude that these proteins may also have some effect. Nonetheless, we were able to confirm that NS1 indeed

potentiates PA-X activity because of a NS1-PA-X functional interaction, and not NS1 itself downregulating luciferase mRNAs. Expression of NS1 alone had no effect on RNA levels (Fig. 6C), even though NS1 alone is able to decrease the protein abundance of eGFP (Fig. 6D). This is consistent with the idea that PR8 NS1 lacks the RNA regulatory function present in some other NS1 variants(45). We were unable to test whether NS1 exerted its potentiating effect by increasing PA-X levels, as we could not reliably detect PA-X-eGFP by western blotting. However, the fact that NS1 decreases eGFP protein levels (Fig. 6D) suggests that there is not a global increase in levels of ectopically expressed proteins in NS1-expressing cells. Overall, this result suggests that during infection, there is a functional interaction between PA-X and NS1 that promotes the host shutoff activity of PA-X, although PA-X can technically function in the absence of additional influenza proteins.

Discussion

Our results reveal that N-terminal acetylation of PA-X supports host shutoff activity in two separate ways: it is required for nuclear localization of PA-X, and it is involved in a second yet undetermined process that promotes PA-X activity. Interestingly, the two processes have slightly different requirements for the modification. Addition of the acetyl group at either the first residue, i.e. the initiator methionine, or the second residue following initiator methionine excision promotes nuclear localization of PA-X. However, mutants that are modified at the second residue, like PA-X E2A, do not downregulate RNA levels, despite being localized to the nucleus. Therefore, the acetyl group on the initiator methionine is specifically required for the full host shutoff activity of PA-X, at least when expressed ectopically. Interestingly, during infection, we found that the retained methionine is not required for the host shutoff activity of PA-X. This restoration of host shutoff activity during infection is due at least in part to the viral protein NS1.

This is the first time that a role for the N-terminal region of PA-X in nuclear localization has been reported. Previous studies have identified charged residues in the C-terminal X-ORF of PA-X that are important for nuclear localization(4,34,35). Here we show that these sequences alone are not enough for PA-X nuclear localization, as they were not mutated in our studies. Conversely, N-terminal acetylation is also not enough to direct PA-X nuclear localization, because the N-terminal domain of PA-X alone does not traffic to the nucleus(4,34,35), even though it is likely still N-terminally acetylated by NatB. The full structure of PA-X with its C-terminal X-ORF has not yet been solved, and further work should determine how the acetylated N-terminus and the C-terminal X-ORF work together to drive the nuclear localization of PA-X.

While N-terminal acetylation has been previously linked to protein localization(29–32,46), this function has generally been confined to membrane localization. This is the first report of regulation of nuclear localization by this modification. N-terminal acetylation directs proteins to membranes through two mechanisms: protein-protein interactions with integral membrane proteins(30,31) and direct interactions with membranes(46). It is possible that the N-terminal acetylation similarly increases binding affinity between PA-X and interacting proteins that mediate nuclear localization. While the details of this effect are still unknown, these results suggest that N-terminal acetylation has a broader range of functions in protein localization than previously reported and mediates interactions with additional trafficking proteins.

How N-terminal acetylation separately mediates the nuclear localization and the host shutoff activity of PA-X remains unclear. Previous studies on N-terminal acetylation have shown that this modification impacts protein-protein interactions(23–26). Biochemically, N-terminal acetylation eliminates the N-terminal positive charge of the first amino acid and increases hydrophobicity. This may allow for a new protein interaction surface that is unavailable when the N-terminus is unmodified. For example, the N-terminally acetylated initiator methionine of the

NEDD8-conjugating E2 enzyme Ubc12 allows for its docking into the hydrophobic pocket of the co-E3 ligase Dcn1, thus promoting the function of the E2/E3 complex(23,24). The structure of the interaction interfaces may also be subtly different depending on whether the initiator methionine is retained. In the case of PA-X, N-terminal acetylation at either the first or second amino acid may support interactions with a cytoplasmic protein that is involved in the nuclear import of PA-X equally well. However, retention of a modified methionine may be needed to create the correct interaction surface for a protein that allows PA-X to reach, bind, and/or degrade its RNA targets in the nucleus. For example, it is possible that while the N-terminally acetylated E2A-modified mutants enter the nucleus, they are unable to then localize to the correct subnuclear compartment to downregulate host mRNAs. These possibilities should be addressed in future studies.

Another open question is how NS1 promotes PA-X host shutoff activity. In addition to our results, a recent study by Bougon et al. supports this idea, as they found some NS1 mutations abolished host shutoff in PR8-infected cells(36). Our results show that PA-X and NS1 do not simply have an additive effect on RNA downregulation, as PR8 NS1 has no effect on RNA levels on its own, as previously reported(47). NS1 binds many host factors(48–54), in some cases causing these proteins to relocalize from nuclear speckles to the nucleoplasm(50). Thus, it is possible that relocalization of a host protein promotes the host shutoff activity of PA-X by facilitating protein-protein interactions in the correct nuclear compartment. It is also possible that NS1 stabilizes these protein interactions. Alternatively, NS1 may promote PA-X host shutoff by preventing host mRNA export from the nucleus. Efficient export of mature mRNAs is coupled to their synthesis by RNA polymerase II and additional processing events(55). In some strains of influenza A virus, NS1 prevents RNA maturation by binding the poly(A) tail and preventing mRNA export from the nucleus to the cytoplasm(56). Our lab has reported that PA-X preferentially downregulates spliced mRNAs that are synthesized by RNA polymerase II(4,5).

Thus, it is possible that PA-X targets are retained in the nucleus by NS1, allowing for an increase in mRNA degradation by PA-X. In addition, we have also shown that PA-X preferentially cleaves GCUG tetramers located in single-stranded regions of hairpin loops(6). As NS1 binds double-stranded RNA(57,58), it could stabilize the hairpin region of PA-X targets, allowing for optimal substrate targeting by PA-X.

While NS1 restores part of PA-X function, it does not explain the whole difference between ectopic expression and infection. Because influenza A virus infection alters the levels of some host proteins(59,60), this change may lead to an increase in PA-X host shutoff activity. In particular, proteins that are associated with protein binding, localization, and transport are upregulated in influenza A virus-infected human lung cells(59). A possible model is that modification of PA-X at the second residue in the NatA-acetylated PA-X E2A mutant results in decreased PA-X binding affinity for an interacting host protein compared to initiator methionine acetylation. However, during infection, this interacting host protein is upregulated, and there is a consequent improvement in its binding to PA-X E2A. This increase in host shutoff activity, alongside the effects that were seen with NS1, could explain the restoration of activity seen during infection. In general, both NS1-dependent and NS1-independent effects of infection on PA-X activity will need to be defined in the future.

Overall, we have discovered that N-terminal acetylation functionally promotes the host shutoff activity of PA-X by separately influencing PA-X subcellular localization and the overall ability of PA-X to downregulate its targets. Our results suggest that acetylation of the initiator methionine specifically promotes RNA downregulation by PA-X. In the future, it will be important to determine how N-terminal acetylation contributes to structural differences and/or PA-X interactions with other proteins and PA-X substrates. Additionally, in the context of cellular

biology, these studies contribute new evidence that N-terminal acetylation supports the correct subcellular localization of modified proteins. To our knowledge, this is also the first report that N-terminal acetylation promotes nuclear localization. Indeed, our studies highlight that N-terminal acetylation is multifaceted in its regulations of modified proteins and that this modification remains incompletely understood, limiting our ability to discern its role in the regulation of proteins in physiological and pathological settings.

Materials and Methods

Plasmids

pCR3.1-PA-X-myc, pCR3.1-PA-X D108A-myc, pCR3.1-PA-X-eGFP, pCR3.1-PA-X D108A-eGFP, pCR3.1-PB2-myc, pCR3.1-PB1-myc, pCR3.1-PA(fs)-myc, pCR3.1-HA-myc, pCR3.1-NP-myc, pCR3.1 NA-myc, pCR3.1-M1-myc, pCR3.1-NS1-myc, and pCR3.1-NEP-myc from the PR8 strain were gifts from C. McCormick (Dalhousie University, Halifax, NS, Canada) and generated as previously described(44). pCDNA3.1-eGFP was a gift from B. Glaunsinger (University of California, Berkley, Berkley, CA, USA). The luciferase construct with the β-globin intron was a gift from G. Dreyfuss (University of Pennsylvania, Philadelphia, PA, USA)(61). The rescue plasmids encoding the 8 segments of PR8 virus (pHW191-PB2 to pHW198-NS) were gifts from R. Webby (St. Jude Children's Research Hospital, Memphis, TN, USA)(62). Gibson cloning using HiFi assembly mix (New England Biolabs) was used to make pCR3.1-PA-X-NLS-eGFP by amplifying the PR8 sequence of PA-X from pCR3.1-PA-X-myc and the eGFP sequence from pCDNA3.1-eGFP. The nuclear localization sequence (NLS) in pCR3.1-PA-X-NLS-eGFP was designed into the primers for Gibson cloning. Similar PA-X-eGFP fusion constructs were made using the PA-Xs from A/Perth/16/2009 H3N2 (Perth) and A/Tennessee/1-560/09 H1N1 (H1N1pdm09). The E2 mutations in the pCR3.1-PA-X-eGFP constructs with PA-Xs from PR8,

Perth, and H1N1pdm09 were generated using the QuikChange II site-directed mutagenesis kit (Agilent). The PR8 pHW-PA(ΔX) plasmid was generated from pHW193 by introducing mutations that reduce frameshifting events and add a premature stop codon in the PA-X reading frame, but that are silent in the PA reading frame, as previously described(5,6).

Cell lines and transfections

Human embryonic kidney (HEK) 293T cells and Madin-Darby canine kidney (MDCK) cells were commercially obtained from ATCC (CRL-3216 and CCL-34, respectively). Both cell lines were maintained in high glucose Dulbecco's modified Eagle's medium (DMEM, Gibco) supplemented with 10% fetal bovine serum (FBS, Cytiva) at 37ºC in 5% CO2 atmosphere. HEK293T cells were plated on 24-well plates and transfected with 500 ng total DNA (including 25 ng PA-X constructs and 50 ng pCMV luciferase + intron construct) in 10% FBS in DMEM using jetPRIME transfection reagent (Polyplus). Cells were collected 24 hours post-transfection for RNA extraction and purification. To determine subcellular localization of PA-X, HEK293T cells were transfected as described above and plated onto poly-L-lysine (Sigma)-treated glass coverslips. To measure the host shutoff activity of PA-X during influenza A virus infections, HEK293Ts were plated in 24-well plates that were pre-treated with fibronection, bovine serum albumin (BSA) and bovine collagen to increase HEK293T adhesion to the plate during the procedure. For the plate treatment, 10 ug/ml fibronectin (Sigma-Aldrich), 100 ug/ml BSA (Sigma-Aldrich), and 30 ug/ml bovine collagen (Advanced Biomatrix) in modified Eagle's medium (MEM, Gibco) were added to the wells and UV crosslinked for 30 minutes. Wells were then washed three times with Dulbecco's phosphate buffered saline (DPBS, Gibco) before addition of the cells. After plating, cells were transfected with 500 ng total DNA (including 25 ng PA-X constructs and 50 ng pCMV luciferase + intron construct) in infection media (0.5% low-endotoxin BSA (Sigma-Aldrich) in high glucose DMEM) using jetPRIME transfection reagent. 8 hours post-transfection, media was

removed and cells were infected as described below. 24 hours post-transfection/16 hours post-infection, cells were collected for RNA extraction and purification.

Viruses and infections

Wild-type influenza A virus A/Puerto Rico/9/1934 H1N1 (PR8) and the mutant recombinant virus PR8 PA(ΔX) were generated using the 8-plasmid reverse genetic system(62) as previously described(4–6). Viral stocks were produced in MDCK cells and infectious titers were determined by plaque assays in MDCK cells using 1.2% Avicel (FMC BioPolymer) overlays(63). Briefly, confluent MDCK cells were infected with low volumes of tenfold serially diluted virus stocks in triplicate for 1 hour. Cells were then washed twice with DPBS before the addition of overlay media (1.2% Avicel, 1X MEM, 0.5% low-endotoxin BSA in DMEM, and 1 ug/ml TPCK-treated trypsin (Sigma-Aldrich)) and incubated for 4 days at 37ºC in 5% CO_2 atmosphere. After 4 days, cells were fixed with 4% paraformaldehyde and stained with crystal violet (Sigma-Aldrich) to observe plaques. Influenza A virus infections following HEK293T transfections were performed in infection media (0.5% low-endotoxin BSA in high glucose DMEM). Briefly, transfected HEK293T cells were treated with infection media supplemented with 0.5 ug/ml TPCK-treated trypsin alone (mock infection) or containing WT PR8 or PR8 PA(ΔX) at a multiplicity of infection (MOI) of 1 and incubated for 16 hours at 37ºC in 5% CO_2 atmosphere. Cells were then collected and lysed in RNA lysis buffer for RNA isolation.

RNA purification, cDNA preparation and qPCR

RNA was extracted and purified using the Quick-RNA miniprep kit (Zymo Research) following the manufacturer's protocol. Purified RNA was treated with Turbo DNase (Life Technologies), then reverse transcribed using iScript supermix (Bio-Rad) per manufacturer's protocol. qPCR was performed using iTaq Universal SYBR Green Supermix (Bio-Rad) on the Bio-Rad CFX Connect Real-Time PCR Detection System or CFX Duet Real-Time PCR System and analyzed

with Bio-Rad CFX Manager software or Bio-Rad CFX Maestro software. Primers used for the qPCR were:

Primer name	**Primer sequence (5' → 3')**
18S forward	GTAACCCGTTGAACCCCATT
18S reverse	CCATCCAATCGGTAGTAGCG
Luciferase forward	ATCGAGGTGGACATTACCTACG
Luciferase reverse	CGCTCGTTGTAGATGTCGTTAG
Human G6PD forward	TGAGCCAGATAGGCTGGAA
Human G6PD reverse	TAACGCAGGCGATGTTGTC
PR8 HA forward	CTGGACCTTGCTAAAACCCG
PR8 HA reverse	TCTGGAAAGGGAGACTGCTG

Confocal microscopy

HEK293T cells were grown on glass coverslips pretreated with poly-L-lysine (Sigma-Aldrich), which were prepared following the manufacturer's protocol. 24 hours after plating, cells were transfected with eGFP-tagged PA-X variants following the protocols described above, cells were washed twice with phosphate buffer saline (PBS) and fixed with 4% paraformaldehyde. Cells were permeabilized in 0.1% Triton X100 and nuclei were stained with 1:10,000 dilution of Hoechst 3342 Fluorescent Stain (Fisher Scientific). Coverslips were then mounted on glass slides using ProLong Gold Antifade Mountant (Thermo Fisher). Images were taken with the Nikon A1R Confocal Microscope or the Leica Stellaris Confocal Microscope. To determine colocalization between the eGFP-tagged PA-X proteins and the nucleus, quantification of fluorescence overlap between eGFP and the nuclear stain was done on at least 10 random

eGFP-positive cells per condition and per replicate experiment using Just Another Colocalization Plugin (JACoP) in ImageJ(38).

Protein collection and western blotting

Cell lysates were prepared using RIPA buffer (50 mM Tris-HCl pH 7.4, 1% NP-40 alternative, 0.5% sodium deoxycholate, 0.1% SDS, 150 mM NaCl, 2 mM EDTA) supplemented with 1X cOmplete EDTA-free protease inhibitor cocktail (Roche), 2 mM $MgCl_2$, and 250 U/ml benzonase nuclease (Sigma-Aldrich). 100 µg of protein were loaded on Mini-PROTEAN® TGX™ Precast Protein Gels, 4–15% (10-well) or Mini-PROTEAN® TGX™ Precast Protein Gels, 4–20% (15 well) SDS-PAGE gels (Bio-Rad) and transferred onto polyvinylidene difluoride (PVDF) membranes (Millipore) using a Trans-Blot Turbo Transfer System (BioRad). Membranes were blocked with 5% milk in Tris buffer saline (TBS) with 0.1% Tween-20 (TBST). Western blots were performed at 4ºC overnight using antibodies against GFP (ChromoTek pabg1-20, 1:500), myc tag (Cell Signaling Technologies #2276, 1:1000) and β-tubulin (Cell Signaling Technologies #2128, 1:1000) diluted in 0.5% milk in TBST for anti-GFP and anti-β-tubulin or 0.5% milk in PBS with 0.1% Tween-20 (PBST) for anti-myc. Secondary antibodies conjugated to horseradish peroxidase (HRP) (Southern biotech) were used at a 1:5000 dilution and a chemiluminescent signal was generated using the Pierce ECL Western Blotting Substrate (Thermo Fisher). Blots were then imaged using an iBright FL1000 Imaging System (iBright Firmware version 1.8.1).

Quantification and statistical analysis

Data are plotted as the mean +/- standard error of the mean and represent three or more independent biological replicates, as shown by the individual data points included in all graphs. Statistical analyses were performed using GraphPad Prism (v10.0.2). For multiple comparisons, one-way analysis of variance (ANOVA) followed by Dunnett's multiple comparison test or two-

way ANOVA followed by uncorrected Fisher's LSD multiple comparison test were used, as indicated in the figure legends. Overall significance was defined as < 0.05. Where indicated, levels of significance are denoted as follows: *p < 0.05, **p < 0.01, ***p < 0.001, ****p < 0.0001.

Acknowledgements

We thank Drs C. McCormick, D. Khaperskyy, B. Glaunsinger, G. Dreyfuss, and R. Webby for constructs. We thank Drs C. McCormick, D. Khaperskyy and members of the Gaglia laboratory for feedback and advice. We thank the Center for Neuroscience Imagining and Cell Analysis Core and Dr. K. Majumder for technical support and assistance on the confocal microscopes used in this study.

Funding

Support for this research was provided by NIH grant R01AI137358 (to MMG), a Rosenberg fellowship from Tufts Graduate School of Biomedical Sciences (to RD) and by the University of Wisconsin-Madison, Office of the Vice Chancellor for Research and Graduate Education with funding from the Wisconsin Alumni Research Foundation. The funders had no role in study design, data collection and analysis, decision to publish, or preparation of the manuscript.

References

1. Jagger BW, Wise HM, Kash JC, Walters KA, Wills NM, Xiao YL, et al. An Overlapping Protein-Coding Region in Influenza A Virus Segment 3 Modulates the Host Response. Science. 2012 Jul 13;337(6091):199–204.

2. Hayashi T, MacDonald LA, Takimoto T. Influenza A Virus Protein PA-X Contributes to Viral Growth and Suppression of the Host Antiviral and Immune Responses. J Virol. 2015 Jun 15;89(12):6442–52.

3. Chaimayo C, Dunagan M, Hayashi T, Santoso N, Takimoto T. Specificity and functional interplay between influenza virus PA-X and NS1 shutoff activity. PLOS Pathog. 2018 Nov 29;14(11):e1007465.

4. Khaperskyy DA, Schmaling S, Larkins-Ford J, McCormick C, Gaglia MM. Selective Degradation of Host RNA Polymerase II Transcripts by Influenza A Virus PA-X Host Shutoff Protein. PLoS Pathog [Internet]. 2016 Feb 5 [cited 2019 Sep 4];12(2). Available from: https://www.ncbi.nlm.nih.gov/pmc/articles/PMC4744033/

5. Gaucherand L, Porter BK, Levene RE, Price EL, Schmaling SK, Rycroft CH, et al. The Influenza A Virus Endoribonuclease PA-X Usurps Host mRNA Processing Machinery to Limit Host Gene Expression. Cell Rep. 2019 Apr;27(3):776-792.e7.

6. Gaucherand L, Iyer A, Gilabert I, Rycroft CH, Gaglia MM. Cut site preference allows influenza A virus PA-X to discriminate between host and viral mRNAs. Nat Microbiol. 2023 Jul;8(7):1304–17.

7. Oishi K, Yamayoshi S, Kozuka-Hata H, Oyama M, Kawaoka Y. N-Terminal Acetylation by NatB Is Required for the Shutoff Activity of Influenza A Virus PA-X. Cell Rep. 2018 Jul 24;24(4):851–60.

8. Brown JL, Roberts WK. Evidence that approximately eighty per cent of the soluble proteins from Ehrlich ascites cells are Nalpha-acetylated. J Biol Chem. 1976 Feb 25;251(4):1009–14.

9. Arnesen T, Van Damme P, Polevoda B, Helsens K, Evjenth R, Colaert N, et al. Proteomics analyses reveal the evolutionary conservation and divergence of N-terminal acetyltransferases from yeast and humans. Proc Natl Acad Sci U S A. 2009 May 19;106(20):8157–62.

10. Aksnes H, Drazic A, Marie M, Arnesen T. First Things First: Vital Protein Marks by N-Terminal Acetyltransferases. Trends Biochem Sci. 2016 Sep 1;41(9):746–60.

11. Aksnes H, Van Damme P, Goris M, Starheim KK, Marie M, Støve SI, et al. An Organellar Nα-Acetyltransferase, Naa60, Acetylates Cytosolic N Termini of Transmembrane Proteins and Maintains Golgi Integrity. Cell Rep. 2015 Mar 3;10(8):1362–74.

12. Starheim KK, Gevaert K, Arnesen T. Protein N-terminal acetyltransferases: when the start matters. Trends Biochem Sci. 2012 Apr 1;37(4):152–61.

13. Ree R, Varland S, Arnesen T. Spotlight on protein N-terminal acetylation. Exp Mol Med. 2018 Jul 27;50(7):90.

14. Arnesen T. Towards a Functional Understanding of Protein N-Terminal Acetylation. PLOS Biol. 2011 May 31;9(5):e1001074.

15. Myklebust LM, Van Damme P, Støve SI, Dörfel MJ, Abboud A, Kalvik TV, et al. Biochemical and cellular analysis of Ogden syndrome reveals downstream Nt-acetylation defects. Hum Mol Genet. 2015 Apr 1;24(7):1956–76.

16. Hwang CS, Shemorry A, Varshavsky A. N-Terminal Acetylation of Cellular Proteins Creates Specific Degradation Signals. Science. 2010 Feb 19;327(5968):973–7.

17. Shemorry A, Hwang CS, Varshavsky A. Control of protein quality and stoichiometries by N-terminal acetylation and the N-end rule pathway. Mol Cell. 2013 May 23;50(4):540–51.

18. Xu F, Huang Y, Li L, Gannon P, Linster E, Huber M, et al. Two N-Terminal Acetyltransferases Antagonistically Regulate the Stability of a Nod-Like Receptor in Arabidopsis. Plant Cell. 2015 May;27(5):1547–62.

19. Sheikh TI, de Paz AM, Akhtar S, Ausió J, Vincent JB. MeCP2_E1 N-terminal modifications affect its degradation rate and are disrupted by the Ala2Val Rett mutation. Hum Mol Genet. 2017 Nov 1;26(21):4132–41.

20. Holmes WM, Mannakee BK, Gutenkunst RN, Serio TR. Loss of amino-terminal acetylation suppresses a prion phenotype by modulating global protein folding. Nat Commun. 2014 Jul 15;5(1):4383.

21. Trexler AJ, Rhoades E. N-terminal acetylation is critical for forming α-helical oligomer of α-synuclein. Protein Sci Publ Protein Soc. 2012 May;21(5):601–5.

22. Bartels T, Choi JG, Selkoe DJ. α-Synuclein occurs physiologically as a helically folded tetramer that resists aggregation. Nature. 2011 Aug 14;477(7362):107–10.

23. Scott DC, Monda JK, Bennett EJ, Harper JW, Schulman BA. N-Terminal Acetylation Acts as an Avidity Enhancer Within an Interconnected Multiprotein Complex. Science. 2011 Nov 4;334(6056):674–8.

24. Monda JK, Scott DC, Miller DJ, Lydeard J, King D, Harper JW, et al. Structural Conservation of Distinctive N-terminal Acetylation-Dependent Interactions across a Family of Mammalian NEDD8 Ligation Enzymes. Structure. 2013 Jan 8;21(1):42–53.

25. Yang D, Fang Q, Wang M, Ren R, Wang H, He M, et al. Nα-acetylated Sir3 stabilizes the conformation of a nucleosome-binding loop in the BAH domain. Nat Struct Mol Biol. 2013 Sep;20(9):1116–8.

26. Arnaudo N, Fernández IS, McLaughlin SH, Peak-Chew SY, Rhodes D, Martino F. The N-terminal acetylation of Sir3 stabilizes its binding to the nucleosome core particle. Nat Struct Mol Biol. 2013 Sep;20(9):1119–21.

27. Singer JM, Shaw JM. Mdm20 protein functions with Nat3 protein to acetylate Tpm1 protein and regulate tropomyosin–actin interactions in budding yeast. Proc Natl Acad Sci U S A. 2003 Jun 24;100(13):7644–9.

28. Coulton AT, East DA, Galinska-Rakoczy A, Lehman W, Mulvihill DP. The recruitment of acetylated and unacetylated tropomyosin to distinct actin polymers permits the discrete regulation of specific myosins in fission yeast. J Cell Sci. 2010 Oct 1;123(19):3235–43.

29. Forte GMA, Pool MR, Stirling CJ. N-Terminal Acetylation Inhibits Protein Targeting to the Endoplasmic Reticulum. PLOS Biol. 2011 May 31;9(5):e1001073.

30. Setty SRG, Strochlic TI, Tong AHY, Boone C, Burd CG. Golgi targeting of ARF-like GTPase Arl3p requires its Nα-acetylation and the integral membrane protein Sys1p. Nat Cell Biol. 2004 May;6(5):414–9.

31. Behnia R, Panic B, Whyte JRC, Munro S. Targeting of the Arf-like GTPase Arl3p to the Golgi requires N-terminal acetylation and the membrane protein Sys1p. Nat Cell Biol. 2004 May;6(5):405–13.

32. Behnia R, Barr FA, Flanagan JJ, Barlowe C, Munro S. The yeast orthologue of GRASP65 forms a complex with a coiled-coil protein that contributes to ER to Golgi traffic. J Cell Biol. 2007 Jan 29;176(3):255–61.

33. Shi M, Jagger BW, Wise HM, Digard P, Holmes EC, Taubenberger JK. Evolutionary Conservation of the PA-X Open Reading Frame in Segment 3 of Influenza A Virus. J Virol. 2012 Nov;86(22):12411–3.

34. Oishi K, Yamayoshi S, Kawaoka Y. Mapping of a Region of the PA-X Protein of Influenza A Virus That Is Important for Its Shutoff Activity. J Virol. 2015 Jun 3;89(16):8661–5.

35. Hayashi T, Chaimayo C, McGuinness J, Takimoto T. Critical Role of the PA-X C-Terminal Domain of Influenza A Virus in Its Subcellular Localization and Shutoff Activity. J Virol. 2016 Aug 15;90(16):7131–41.

36. Bougon J, Kadijk E, Gallot-Lavallee L, Curtis B, Landers M, Archibald JM, et al. Influenza A virus NS1 effector domain is required for PA-X mediated host shutoff [Internet]. bioRxiv; 2023 [cited 2023 Dec 1]. p. 2023.10.02.560421. Available from: https://www.biorxiv.org/content/10.1101/2023.10.02.560421v1

37. Goetze S, Qeli E, Mosimann C, Staes A, Gerrits B, Roschitzki B, et al. Identification and Functional Characterization of N-Terminally Acetylated Proteins in Drosophila melanogaster. PLOS Biol. 2009 Nov 3;7(11):e1000236.

38. Bolte S, Cordelières FP. A guided tour into subcellular colocalization analysis in light microscopy. J Microsc. 2006 Dec;224(Pt 3):213–32.

39. Adam SA, Lobl TJ, Mitchell MA, Gerace L. Identification of specific binding proteins for a nuclear location sequence. Nature. 1989 Jan;337(6204):276–9.

40. Wingfield P. N-Terminal Methionine Processing. Curr Protoc Protein Sci. 2017 Apr 3;88:6.14.1-6.14.3.

41. Van Damme P. Charting the N-Terminal Acetylome: A Comprehensive Map of Human NatA Substrates. Int J Mol Sci. 2021 Oct 2;22(19):10692.

42. Levene RE, Shrestha SD, Gaglia MM. The Influenza A Virus Host Shutoff Factor PA-X Is Rapidly Turned Over in a Strain-Specific Manner. J Virol. 95(8):e02312-20.

43. CDC. Centers for Disease Control and Prevention. 2023 [cited 2023 Dec 1]. Weekly U.S. Influenza Surveillance Report. Available from: https://www.cdc.gov/flu/weekly/index.htm

44. Khaperskyy DA, Emara MM, Johnston BP, Anderson P, Hatchette TF, McCormick C. Influenza A Virus Host Shutoff Disables Antiviral Stress-Induced Translation Arrest. PLoS Pathog. 2014 Jul 10;10(7):e1004217.

45. Levene RE, Gaglia MM. Host Shutoff in Influenza A Virus: Many Means to an End. Viruses. 2018 Sep 5;10(9):475.

46. Dikiy I, Eliezer D. N-terminal acetylation stabilizes N-terminal helicity in lipid- and micelle-bound α-synuclein and increases its affinity for physiological membranes. J Biol Chem. 2014 Feb 7;289(6):3652–65.

47. Salvatore M, Basler CF, Parisien JP, Horvath CM, Bourmakina S, Zheng H, et al. Effects of Influenza A Virus NS1 Protein on Protein Expression: the NS1 Protein Enhances Translation and Is Not Required for Shutoff of Host Protein Synthesis. J Virol. 2002 Feb;76(3):1206–12.

48. Koliopoulos MG, Lethier M, van der Veen AG, Haubrich K, Hennig J, Kowalinski E, et al. Molecular mechanism of influenza A NS1-mediated TRIM25 recognition and inhibition. Nat Commun. 2018 May 8;9:1820.

49. Hale BG, Jackson D, Chen YH, Lamb RA, Randall RE. Influenza A virus NS1 protein binds p85β and activates phosphatidylinositol-3-kinase signaling. Proc Natl Acad Sci U S A. 2006 Sep 19;103(38):14194–9.

50. Chen Z, Li Y, Krug RM. Influenza A virus NS1 protein targets poly(A)-binding protein II of the cellular 3'-end processing machinery. EMBO J. 1999 Apr 15;18(8):2273–83.

51. Das K, Ma LC, Xiao R, Radvansky B, Aramini J, Zhao L, et al. Structural basis for suppression of a host antiviral response by influenza A virus. Proc Natl Acad Sci U S A. 2008 Sep 2;105(35):13093–8.

52. Chien C ya, Xu Y, Xiao R, Aramini JM, Sahasrabudhe PV, Krug RM, et al. Biophysical Characterization of the Complex between Double-Stranded RNA and the N-Terminal Domain of the NS1 Protein from Influenza A Virus: Evidence for a Novel RNA-Binding Mode. Biochemistry. 2004 Feb 1;43(7):1950–62.

53. Burgui I, Aragón T, Ortín J, Nieto A. PABP1 and eIF4GI associate with influenza virus NS1 protein in viral mRNA translation initiation complexes. J Gen Virol. 2003;84(12):3263–74.

54. Aragón T, de la Luna S, Novoa I, Carrasco L, Ortín J, Nieto A. Eukaryotic Translation Initiation Factor 4GI Is a Cellular Target for NS1 Protein, a Translational Activator of Influenza Virus. Mol Cell Biol. 2000 Sep;20(17):6259–68.

55. Lee KM, Tarn WY. Coupling pre-mRNA processing to transcription on the RNA factory assembly line. RNA Biol. 2013 Mar 1;10(3):380–90.

56. Qiu Y, Krug RM. The influenza virus NS1 protein is a poly(A)-binding protein that inhibits nuclear export of mRNAs containing poly(A). J Virol. 1994 Apr;68(4):2425–32.

57. Min JY, Krug RM. The primary function of RNA binding by the influenza A virus NS1 protein in infected cells: Inhibiting the 2′-5′ oligo (A) synthetase/RNase L pathway. Proc Natl Acad Sci U S A. 2006 May 2;103(18):7100–5.

58. Lu Y, Qian XY, Krug RM. The influenza virus NS1 protein: a novel inhibitor of pre-mRNA splicing. Genes Dev. 1994 Aug 1;8(15):1817–28.

59. Coombs KM, Berard A, Xu W, Krokhin O, Meng X, Cortens JP, et al. Quantitative Proteomic Analyses of Influenza Virus-Infected Cultured Human Lung Cells. J Virol. 2010 Oct 15;84(20):10888–906.

60. Haas KM, McGregor MJ, Bouhaddou M, Polacco BJ, Kim EY, Nguyen TT, et al. Proteomic and genetic analyses of influenza A viruses identify pan-viral host targets. Nat Commun. 2023 Sep 27;14(1):6030.

61. Younis I, Berg M, Kaida D, Dittmar K, Wang C, Dreyfuss G. Rapid-Response Splicing Reporter Screens Identify Differential Regulators of Constitutive and Alternative Splicing. Mol Cell Biol. 2010 Apr;30(7):1718–28.

62. Hoffmann E, Krauss S, Perez D, Webby R, Webster RG. Eight-plasmid system for rapid generation of influenza virus vaccines. Vaccine. 2002 Aug 19;20(25):3165–70.

63. Matrosovich M, Matrosovich T, Garten W, Klenk HD. New low-viscosity overlay medium for viral plaque assays. Virol J. 2006 Aug 31;3:63.

Figure legends

Fig 1. N-terminal acetylation of PA-X is required for nuclear localization. (A) Diagram showing which Nat complexes acetylate nascent proteins depending on the first two amino acids. WT PA-X and the PA-X E2 mutants E2D and E2N are modified by NatB (purple), PA-X E2L and E2M mutants are modified by NatC (yellow), and PA-X E2A, E2S, and E2V mutants are modified by NatA (blue). The PA-X E2P mutant should be unmodified. (B-G) HEK293T cells were transfected for 24 hours with empty vector, WT PR8 PA-X-eGFP, the catalytically inactive PA-X D108A-eGFP mutant, or the indicated PR8 PA-X-eGFP mutants carrying changes in the second amino acid. For B, a PR8 PA-X E2P mutant carrying an SV40 nuclear localization sequence (PA-X E2P-NLS-eGFP) was also transfected. (B,E) mRNA levels of a co-transfected luciferase reporter were measured by RT-qPCR and normalized to 18S rRNA. Levels are plotted as change relative to vector transfected cells. (C,F) Confocal microscopy was used to image eGFP-positive cells. Nuclei are stained with Hoechst. Representative images are shown. (D,G) Manders' overlap coefficients for colocalization of nuclei and GFP signal on images were determined using JACoP in ImageJ. Each data point represents 10-15 eGFP positive cells. Manders' overlap coefficient values represent the following localization: ~1: all protein is nuclear; ~0.5: protein is diffuse throughout the cell.

Error bars indicate the standard error of the mean. *$p < 0.05$, **$p < 0.01$, ***$p < 0.001$, ****$p < 0.0001$, ANOVA with Dunnett's multiple comparison test compared to wild-type PA-X.

Fig 2. General N-terminal acetylation is sufficient for PA-X localization to the nucleus. HEK293T cells were transfected for 24 hours with empty vector, WT PR8 PA-X-eGFP, the catalytically inactive PA-X D108A-eGFP mutant, or the indicated NatA-modified PR8 PA-X-eGFP mutants carrying changes in the second amino acid. (A) mRNA levels of a co-transfected luciferase reporter were measured by RT-qPCR and normalized to 18S rRNA. Levels are plotted as change relative to vector transfected cells. (B) Confocal microscopy was used to

image eGFP, PA-X-eGFP (PA-X), PA-X E2A-eGFP (E2A), PA-X E2S-eGFP (E2S), and PA-X E2V-eGFP (E2V). Nuclei were stained with Hoechst. Representative images are shown. (C) Manders' overlap coefficients for colocalization of nuclei and eGFP signal were determined on images using JACoP in ImageJ, where each point represents 10-15 eGFP-positive cells. Manders' overlap coefficient values represent the following localization: ~1: all protein is nuclear; ~0.5: protein is diffuse throughout the cell.

Error bars indicate the standard error of the mean. *p < 0.05, **p < 0.01, ***p < 0.001, ****p < 0.0001, ANOVA with Dunnett's multiple comparison test compared to wild-type PA-X.

Fig 3. N-terminal acetylation at the initiator methionine promotes PA-X host shutoff activity. HEK293T cells were transfected for 24 hours with empty vector, WT PR8 PA-X-eGFP, the catalytically inactive PA-X D108A-eGFP mutant, or the indicated NatC-modified PR8 PA-X-eGFP mutants carrying changes in the second amino acid. (A) mRNA levels of a co-transfected luciferase reporter were measured by RT-qPCR and normalized to 18S rRNA. Levels are plotted as change relative to vector transfected cells. (B) Confocal microscopy was used to image eGFP, PA-X-eGFP (PA-X), PA-X E2M-eGFP (E2M), and PA-X E2L-eGFP (E2L). Nuclei were stained with Hoechst. Representative images are shown. (C) Manders' overlap coefficients for colocalization of nuclei and eGFP signal were determined on images using JACoP in ImageJ, where each point represents 10-15 eGFP-positive cells. Manders' overlap coefficient values represent the following localization: ~1: all protein is nuclear; ~0.5: protein is diffuse throughout the cell.

Error bars indicate the standard error of the mean. *p < 0.05, **p < 0.01, ***p < 0.001, ****p < 0.0001, ANOVA with Dunnett's multiple comparison test compared to wild-type PA-X.

Fig 4. N-terminal acetylation also regulates the activity of PA-X proteins from circulating influenza A virus subtypes. HEK293T cells were transfected for 24 hours with empty vector,

WT PR8 PA-X-eGFP, WT H1N1pdm09 PA-X-eGFP, or WT Perth PA-X-eGFP or the indicated PR8 PA-X-eGFP mutants carrying changes in the second amino acid. mRNA levels of a co-transfected luciferase reporter were measured by RT-qPCR and normalized to 18S rRNA. Levels are plotted as change relative to vector transfected cells. Error bars indicate the standard error of the mean. *p < 0.05, **p < 0.01, ***p < 0.001, ****p < 0.0001, ANOVA with Dunnett's multiple comparison test compared to wild-type PA-X.

Fig 5. During infection, N-terminal acetylation of PA-X at any position is sufficient for host shutoff activity. HEK293T cells were transfected for 24 hours with empty vector, eGFP, and eGFP-tagged WT PA-X, or the following eGFP-tagged mutants: unmodified mutant PA-X E2P (gray), NatB-modified PA-X E2D mutant (purple), NatA-modified mutant E2A (blue), or NatC-modified mutant E2M (yellow). Eight hours post-transfection, cells were mock infected or infected with WT PR8 or the PA-X deficient PR8 PA(ΔX) virus at an MOI of 1. RNA samples were collected 16 hrs post-infection (24 hrs post-transfection). mRNA levels of (A) viral HA mRNA, (B) endogenous G6PD mRNA, and (C) the co-transfected luciferase reporter were measured by RT-qPCR and normalized to 18S rRNA. For B,C, levels are plotted as change relative to vector transfected cells. For C, significance is calculated in comparison to RNA levels in WT PA-X-transfected cells within each infection condition. *p < 0.05, **p < 0.01, ***p < 0.001, ****p < 0.0001 Ordinary two-way ANOVA with uncorrected Fisher's LSD multiple comparison test compared to the wild-type PA-X in each infection condition.

Fig 6. Influenza A virus protein NS1 potentiates PA-X activity. (A,B) Protein and RNA were collected from HEK293T cells that were transfected for 24 hours with empty vector, WT PA-X-eGFP, the NatA-modified mutant PA-X E2A-eGFP, or PA-X E2A-eGFP together with myc-tagged versions of the indicated proteins. (A) mRNA levels of a co-transfected luciferase reporter were measured by RT-qPCR and normalized to 18S rRNA. Levels are plotted as

change relative to vector transfected cells. (B) Production of the PR8 proteins was analyzed by western blotting using an antibody against the myc tag, with tubulin as a loading control. (C,D) Protein and RNA were collected from HEK293T cells that were transfected for 24 hours with empty vector, eGFP, WT PA-X-eGFP, the NatA-modified mutant PA-X E2A-eGFP, myc-tagged PR8 NS1 or a combination of these constructs. (C) mRNA levels of a co-transfected luciferase reporter were measured by RT-qPCR and normalized to 18S rRNA. Levels are plotted as change relative to vector transfected cells. (D) Protein levels were analyzed by western blotting using an myc antibody for myc-tagged NS1, a GFP antibody for eGFP (eGFP-tagged PA-X was not detected in these lysates, despite clear mRNA downregulation in C), and a tubulin antibody as a loading control.

Western blot images are representative of 3 independent biological replicates. Error bars indicate the standard error of the mean. *$p < 0.05$, **$p < 0.01$, ***$p < 0.001$, ****$p < 0.0001$, ANOVA with Dunnett's multiple comparison test compared to WT PA-X.

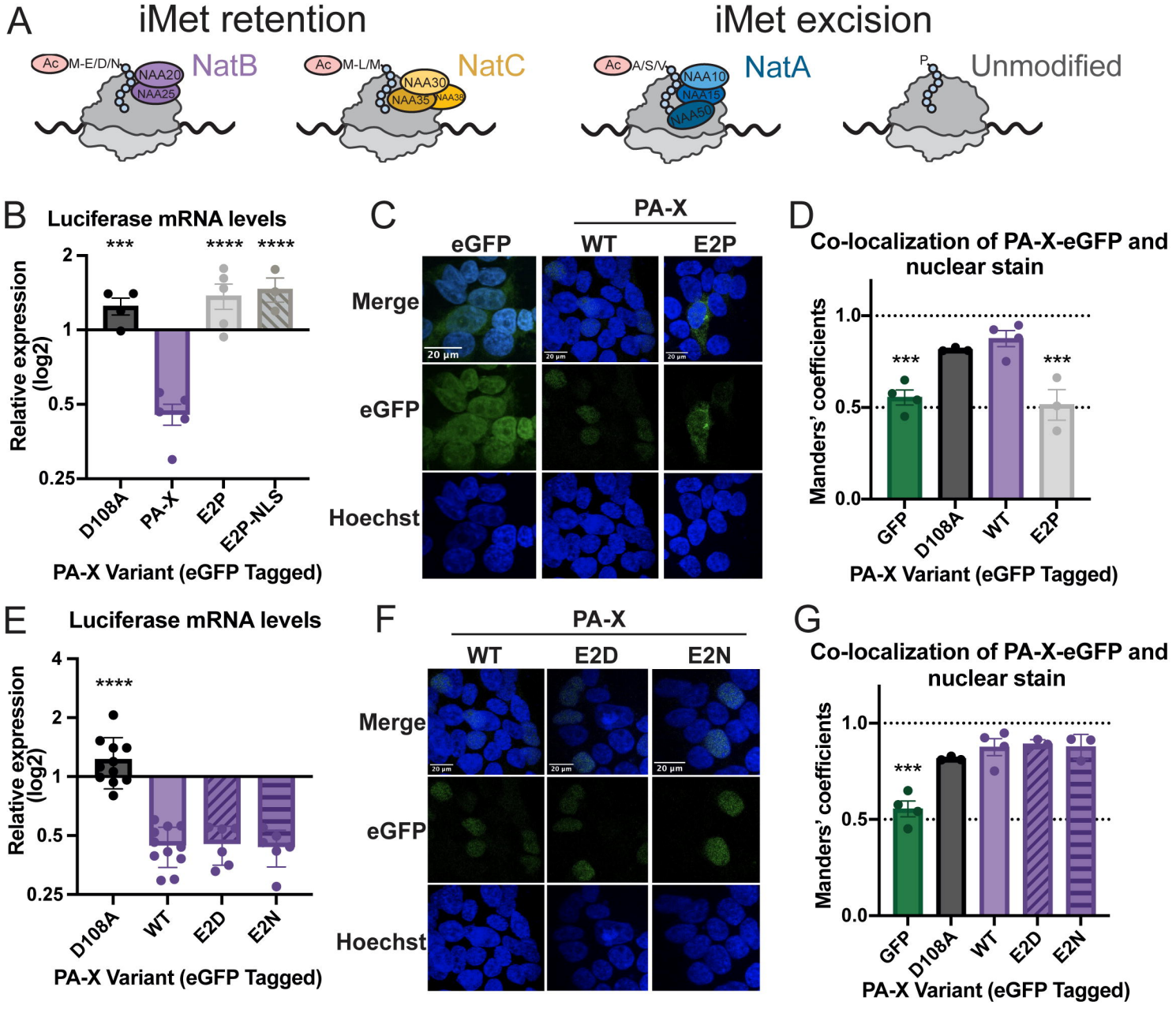

Fig 1. N-terminal acetylation of PA-X is required for nuclear localization. (A) Diagram showing which Nat complexes acetylate nascent proteins depending on the first two amino acids. WT PA-X and the PA-X E2 mutants E2D and E2N are modified by NatB (purple), PA-X E2L and E2M mutants are modified by NatC (yellow), and PA-X E2A, E2S, and E2V mutants are modified by NatA (blue). The PA-X E2P mutant should be unmodified. (B-G) HEK293T cells were transfected for 24 hours with empty vector, WT PR8 PA-X-eGFP, the catalytically inactive PA-X D108A-eGFP mutant, or the indicated PR8 PA-X-eGFP mutants carrying changes in the second amino acid. For B, a PR8 PA-X E2P mutant carrying an SV40 nuclear localization sequence (PA-X E2P-NLS-eGFP) was also transfected. (B,E) mRNA levels of a co-transfected luciferase reporter were measured by RT-qPCR and normalized to 18S rRNA. Levels are plotted as change relative to vector transfected cells. (C,F) Confocal microscopy was used to image eGFP-positive cells. Nuclei are stained with Hoechst. Representative images are shown. (D,G) Manders' overlap coefficients for colocalization of nuclei and GFP signal on images were determined using JACoP in ImageJ. Each data point represents 10-15 eGFP positive cells. Manders' overlap coefficient values represent the following localization: ~1: all protein is nuclear; ~0.5: protein is diffuse throughout the cell.
Error bars indicate the standard error of the mean. *$p < 0.05$, **$p < 0.01$, ***$p < 0.001$, ****$p < 0.0001$, ANOVA with Dunnett's multiple comparison test compared to wild-type PA-X.

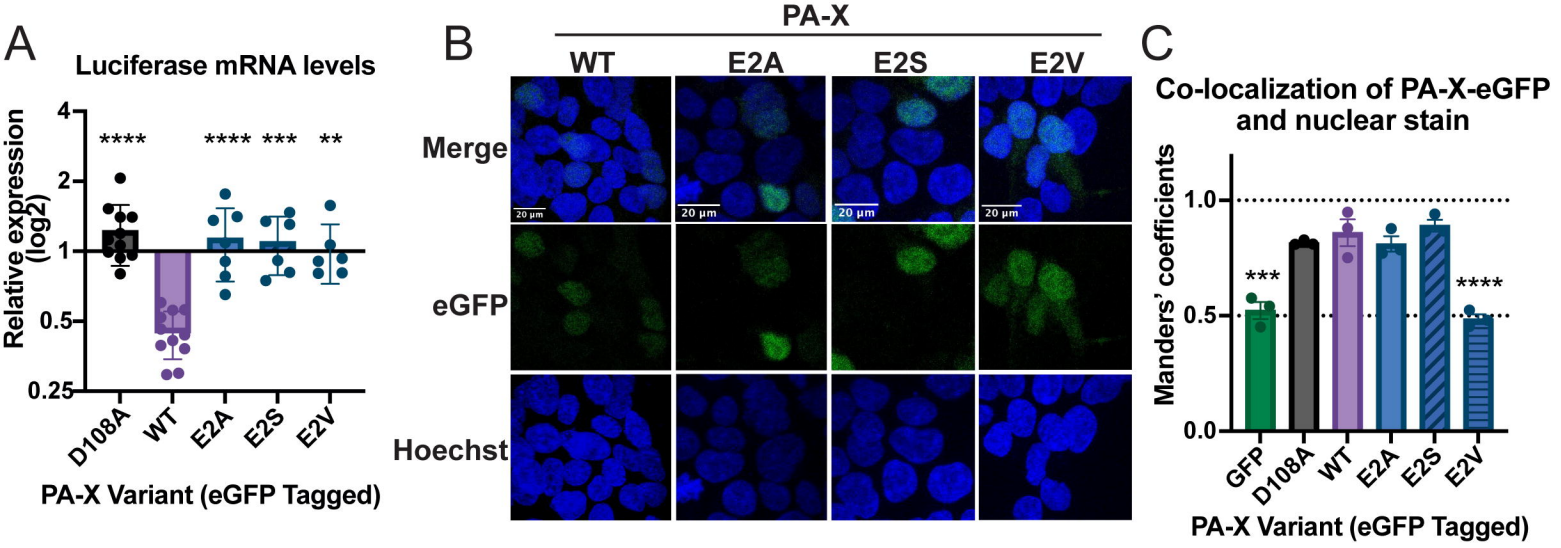

Fig 2. General N-terminal acetylation is sufficient for PA-X localization to the nucleus. HEK293T cells were transfected for 24 hours with empty vector, WT PR8 PA-X-eGFP, the catalytically inactive PA-X D108A-eGFP mutant, or the indicated NatA-modified PR8 PA-X-eGFP mutants carrying changes in the second amino acid. (A) mRNA levels of a co-transfected luciferase reporter were measured by RT-qPCR and normalized to 18S rRNA. Levels are plotted as change relative to vector transfected cells. (B) Confocal microscopy was used to image eGFP, PA-X-eGFP (PA-X), PA-X E2A-eGFP (E2A), PA-X E2S-eGFP (E2S), and PA-X E2V-eGFP (E2V). Nuclei were stained with Hoechst. Representative images are shown. (C) Manders' overlap coefficients for colocalization of nuclei and eGFP signal were determined on images using JACoP in ImageJ, where each point represents 10-15 eGFP-positive cells. Manders' overlap coefficient values represent the following localization: ~1: all protein is nuclear; ~0.5: protein is diffuse throughout the cell.

Error bars indicate the standard error of the mean. *$p < 0.05$, **$p < 0.01$, ***$p < 0.001$, ****$p < 0.0001$, ANOVA with Dunnett's multiple comparison test compared to wild-type PA-X.

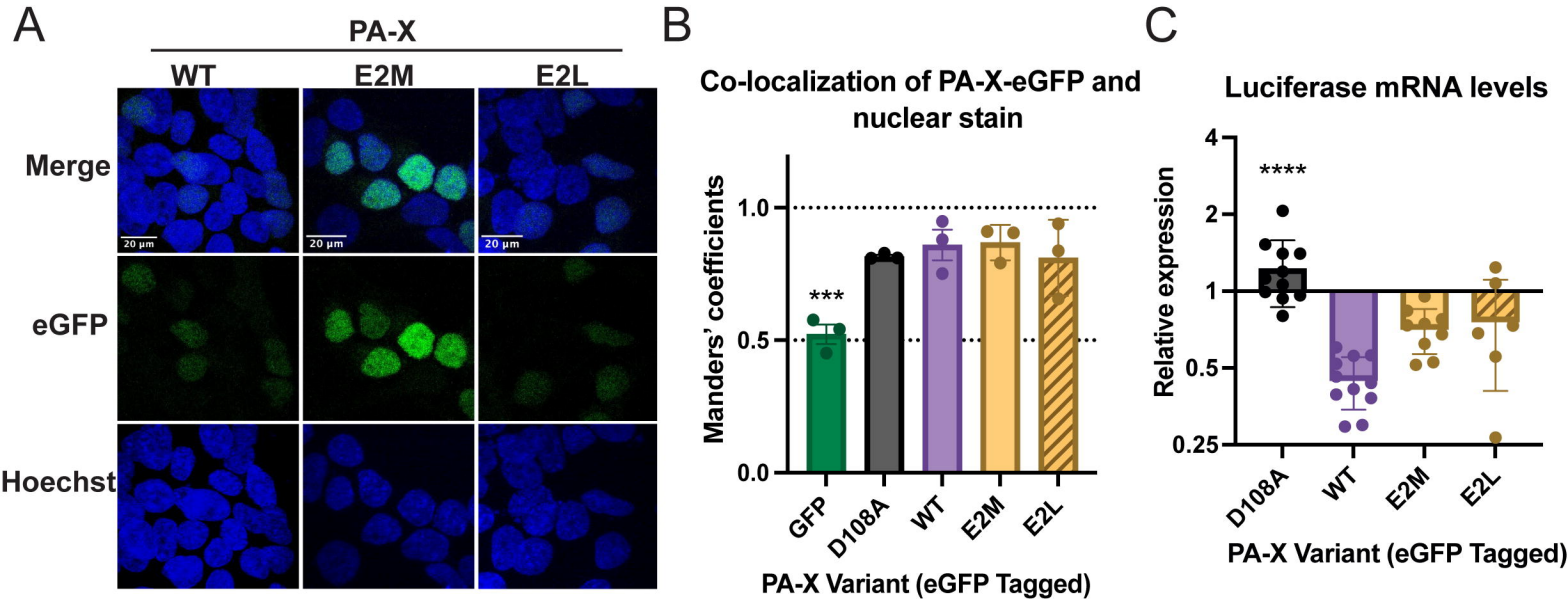

Fig 3. N-terminal acetylation at the initiator methionine promotes PA-X host shutoff activity. HEK293T cells were transfected for 24 hours with empty vector, WT PR8 PA-X-eGFP, the catalytically inactive PA-X D108A-eGFP mutant, or the indicated NatC-modified PR8 PA-X-eGFP mutants carrying changes in the second amino acid. (A) mRNA levels of a co-transfected luciferase reporter were measured by RT-qPCR and normalized to 18S rRNA. Levels are plotted as change relative to vector transfected cells. (B) Confocal microscopy was used to image eGFP, PA-X-eGFP (PA-X), PA-X E2M-eGFP (E2M), and PA-X E2L-eGFP (E2L). Nuclei were stained with Hoechst. Representative images are shown. (C) Manders' overlap coefficients for colocalization of nuclei and eGFP signal were determined on images using JACoP in ImageJ, where each point represents 10-15 eGFP-positive cells. Manders' overlap coefficient values represent the following localization: ~1: all protein is nuclear; ~0.5: protein is diffuse throughout the cell.
Error bars indicate the standard error of the mean. *$p < 0.05$, **$p < 0.01$, ***$p < 0.001$, ****$p < 0.0001$, ANOVA with Dunnett's multiple comparison test compared to wild-type PA-X.

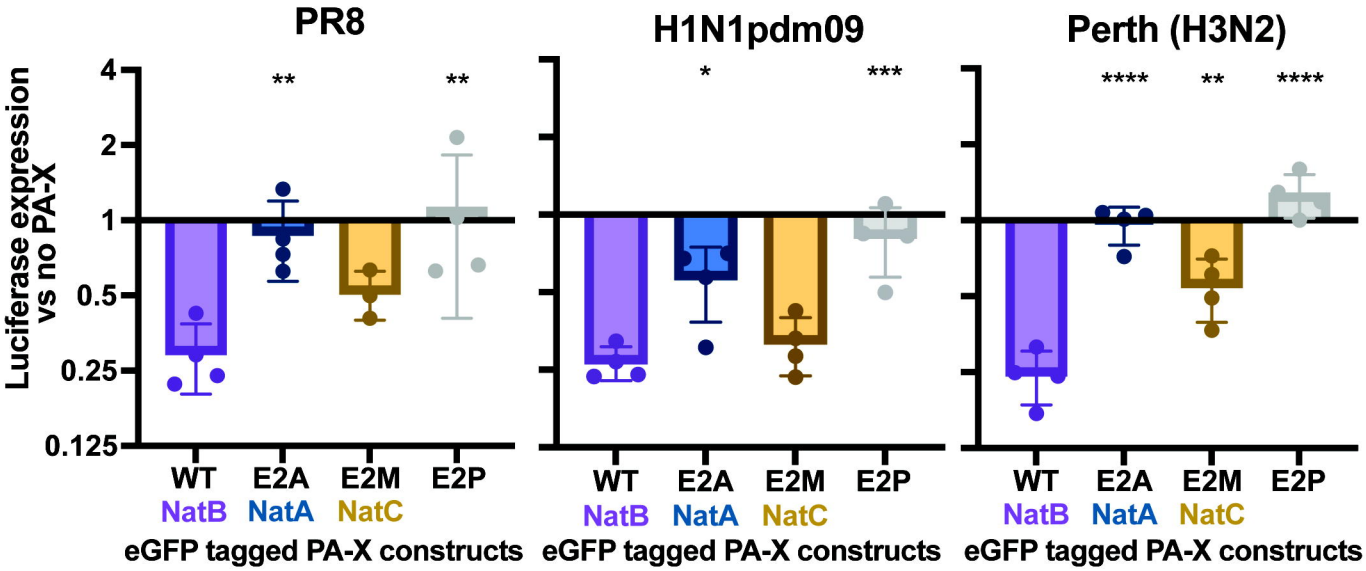

Fig 4. N-terminal acetylation also regulates the activity of PA-X proteins from circulating influenza A virus subtypes. HEK293T cells were transfected for 24 hours with empty vector, WT PR8 PA-X-eGFP, WT H1N1pdm09 PA-X-eGFP, or WT Perth PA-X-eGFP or the indicated PR8 PA-X-eGFP mutants carrying changes in the second amino acid. mRNA levels of a co-transfected luciferase reporter were measured by RT-qPCR and normalized to 18S rRNA. Levels are plotted as change relative to vector transfected cells. Error bars indicate the standard error of the mean. *$p < 0.05$, **$p < 0.01$, ***$p < 0.001$, ****$p < 0.0001$, ANOVA with Dunnett's multiple comparison test compared to wild-type PA-X.

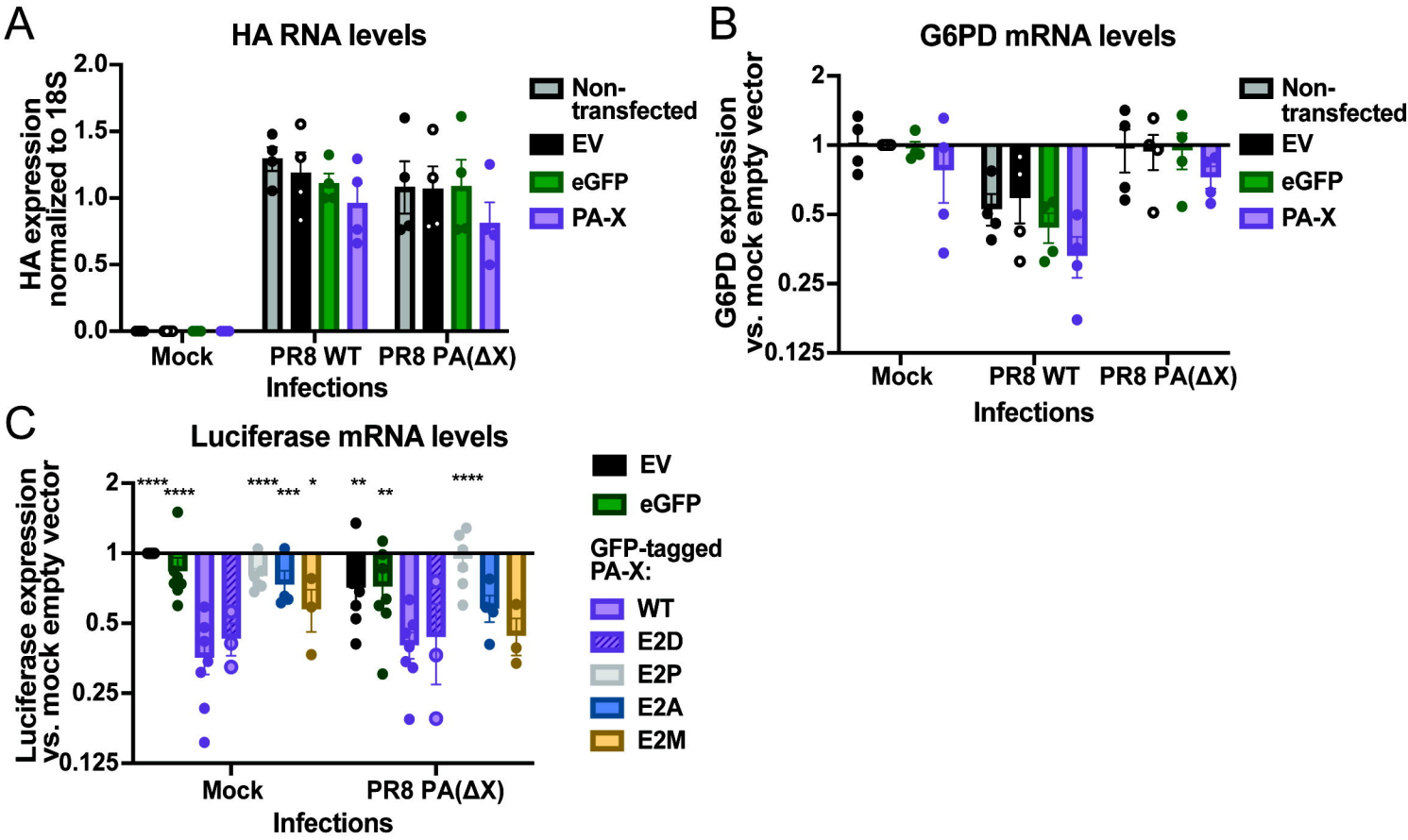

Fig 5. During infection, N-terminal acetylation of PA-X at any position is sufficient for host shutoff activity. HEK293T cells were transfected for 24 hours with empty vector, eGFP, and eGFP-tagged WT PA-X, or the following eGFP-tagged mutants: unmodified mutant PA-X E2P (gray), NatB-modified PA-X E2D mutant (purple), NatA-modified mutant E2A (blue), or NatC-modified mutant E2M (yellow). Eight hours post-transfection, cells were mock infected or infected with WT PR8 or the PA-X deficient PR8 PA(ΔX) virus at an MOI of 1. RNA samples were collected 16 hrs post-infection (24 hrs post-transfection). mRNA levels of (A) viral HA mRNA, (B) endogenous G6PD mRNA, and (C) the co-transfected luciferase reporter were measured by RT-qPCR and normalized to 18S rRNA. For B,C, levels are plotted as change relative to vector transfected cells. For C, significance is calculated in comparison to RNA levels in WT PA-X-transfected cells within each infection condition. *$p < 0.05$, **$p < 0.01$, ***$p < 0.001$, ****$p < 0.0001$ Ordinary two-way ANOVA with uncorrected Fisher's LSD multiple comparison test compared to the wild-type PA-X in each infection condition.

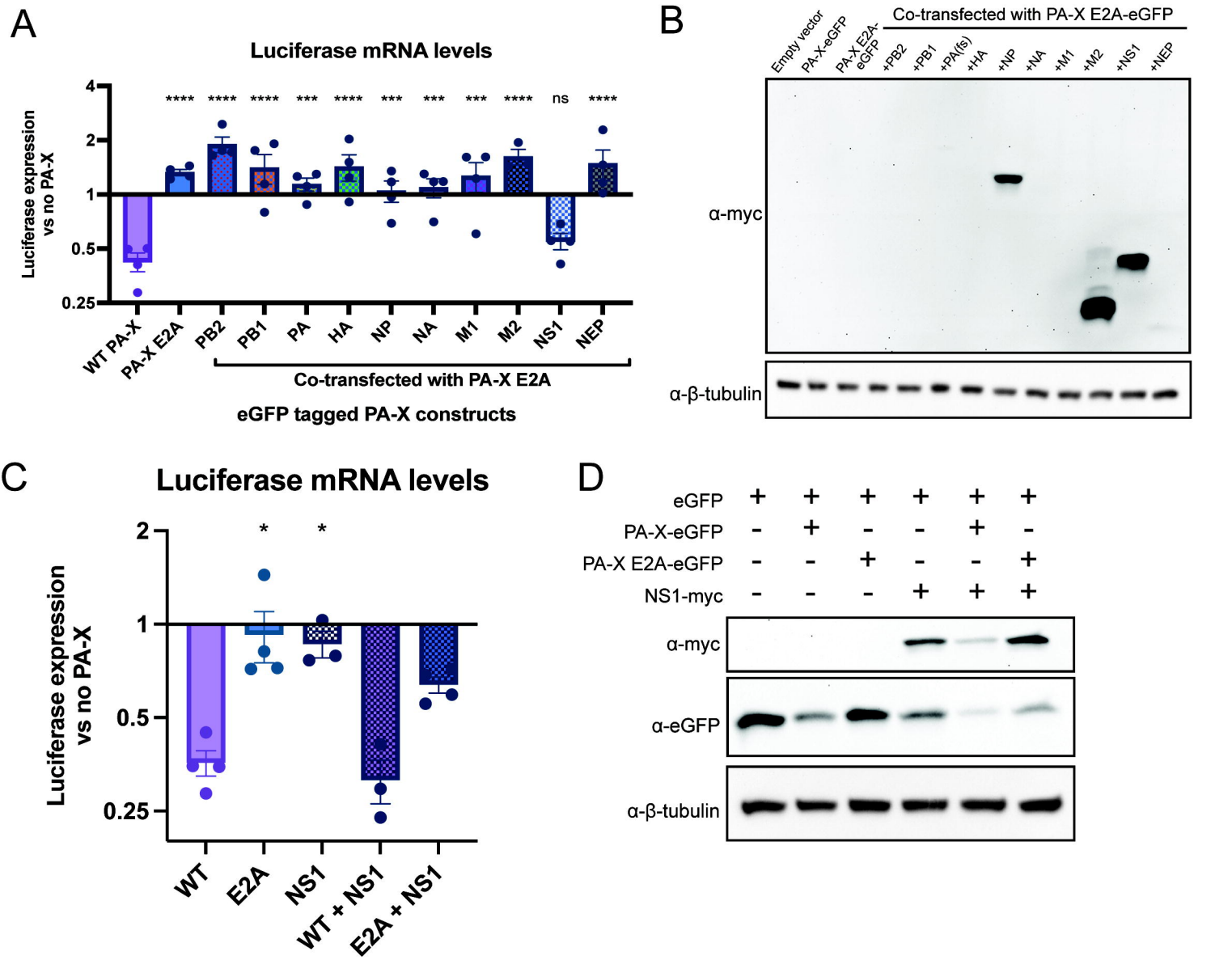

Fig 6. Influenza A virus protein NS1 potentiates PA-X activity. (A,B) Protein and RNA were collected from HEK293T cells that were transfected for 24 hours with empty vector, WT PA-X-eGFP, the NatA-modified mutant PA-X E2A-eGFP, or PA-X E2A-eGFP together with myc-tagged versions of the indicated proteins. (A) mRNA levels of a co-transfected luciferase reporter were measured by RT-qPCR and normalized to 18S rRNA. Levels are plotted as change relative to vector transfected cells. (B) Production of the PR8 proteins was analyzed by western blotting using an antibody against the myc tag, with tubulin as a loading control. (C,D) Protein and RNA were collected from HEK293T cells that were transfected for 24 hours with empty vector, eGFP, WT PA-X-eGFP, the NatA-modified mutant PA-X E2A-eGFP, myc-tagged PR8 NS1 or a combination of these constructs. (C) mRNA levels of a co-transfected luciferase reporter were measured by RT-qPCR and normalized to 18S rRNA. Levels are plotted as change relative to vector transfected cells. (D) Protein levels were analyzed by western blotting using an myc antibody for myc-tagged NS1, a GFP antibody for eGFP (eGFP-tagged PA-X was not detected in these lysates, despite clear mRNA downregulation in C), and a tubulin antibody as a loading control. Western blot images are representative of 3 independent biological replicates. Error bars indicate the standard error of the mean. *$p < 0.05$, **$p < 0.01$, ***$p < 0.001$, ****$p < 0.0001$, ANOVA with Dunnett's multiple comparison test compared to WT PA-X.